Spectroscopic imaging of the secondary star in AM Her

Article (Published Version)

Mon. Not. R. Astron. Soc. **280,** 481–488 (1996)

Spectroscopic imaging of the secondary star in AM Her

Stephen C. Davey and Robert Connon Smith

Astronomy Centre, School of Mathematical and Physical Sciences, University of Sussex, Falmer, Brighton BN1 9QH

Accepted 1995 December 1. Received 1995 November 29; in original form 1994 September 29

ABSTRACT

Spectroscopic observations of AM Her are used to determine the orbital velocity of the secondary star. We describe how the radial velocities and flux deficits derived from the Na I doublet around 8190 Å can be used to map the Na I surface distribution and hence give an estimate of K_2, corrected for the effects of irradiation. The resulting surface maps are consistent with the accretion geometry proposed by Cropper and, from the 'quality' of the fit, suggest an inclination of 50° or more, higher than that normally quoted.

Key words: binaries: spectroscopic – stars: fundamental parameters – stars: individual: AM Her – novae, cataclysmic variables.

1 INTRODUCTION

AM Her is the prototypical magnetic cataclysmic variable (CV), a class which now includes both polars (also called AM Hers) and intermediate polars. Unlike other CVs, AM Her stars are believed to have no accretion discs, and material falls from the secondary star along the magnetic field lines of the white dwarf. Because of the strong magnetic field the white dwarf star rotates synchronously with the orbital period; this distinguishes the AM Hers from intermediate polars, whose white dwarfs rotate much faster than the orbital period, and which may have discs.

Since there is no disc, the spectrum of the faint secondary is often detectable. The Na I doublet around 8190 Å has been observed in several AM Her systems and it provides important radial velocity information about the secondary star, which helps to constrain system parameters. However, when determinations are made of the orbital velocity of the secondary star, K_2, it is necessary to make corrections for geometrical distortion and for irradiation by the primary star and the accretion flow. The purpose of this paper is to apply spectroscopic imaging techniques to make these corrections, and thus to determine K_2 and other parameters for AM Her.

2 THE SURFACE IMAGING METHOD

2.1 Residual radial velocities

The spectra of AM Her were taken on 1986 June 21 and 22 by Martin, Smith and Jones (Martin 1988; see also Friend et al. 1988, Davey & Smith 1992 and Southwell et al. 1995). They measured radial velocities from the Na I line and obtained $K_{abs} = 199.3 \pm 2.0$ km s^{-1} and an eccentricity of 0.068 ± 0.010. This eccentricity was significant at the 99 per cent level, implying that the radial velocity of the secondary, K_{abs}, derived from the absorption-line measurements, would have to be corrected to obtain the true orbital velocity, K_2.

If the orbit were circular, the motion of the centre of mass of the secondary star would be given by

$$V(\varphi) = \gamma + K_2 \sin(2\pi\varphi), \quad (1)$$

where γ is the systemic velocity, and φ is the phase angle of the observation, with $\varphi = 0.0$ at inferior conjunction of the secondary star, i.e., when the red dwarf is in front of the white dwarf. Since cataclysmic binary systems have very short periods, it is generally believed that any initial non-circularity would have been removed rapidly by tidal forces between the red dwarf and the white dwarf, and that the present orbits would indeed be circular. However, the radial velocity curve could still be distorted from a pure sine wave by geometrical distortion and heating of the secondary star by its companion, causing the centre of light given by the strength of the Na I doublet to differ from the centre of mass. We assume here that the measured eccentricity arises from this effect.

In our earlier paper (Davey & Smith 1992), we began the process of correcting for irradiation by making an initial estimate of the true value of K_2. The sine curve given by equation (1), which is from the orbital motion of the secondary star, was then subtracted from the observed radial velocities. This removes the large dynamical contribution to the radial velocity curve and reveals the much smaller contribution due to irradiation.

2.2 Finding the surface map

The next step is to construct a surface irradiation map that is able to fit these residual velocities. This work uses the simulation program by J. S. Martin (Martin 1988; Martin et al. 1989) to produce model radial velocities. Originally, the program was designed to calculate the radial velocity curve for a given irradiation model. With the surface mapping approach, we instead look for the Na I doublet line strength distribution that is consistent with the observations, and only later consider what irradiation model could reproduce the observed map.

Because we are trying to calculate a 2D surface map from a 1D velocity curve, it is necessary to make some assumption about the surface distribution. As a simple first approach, we adopted a 'one-spot' model, where we assume that there is one region on the star that is being heated and that it is the position and size of this region that is to be found. Because the radial velocity data will typically constrain the equatorial distribution much better than the latitudinal variation (e.g. Collier Cameron 1992), we adopt a simple $\sin\theta$ dependence for the variation with latitude, and use the model to determine the longitudinal variation. This tacitly assumes symmetry about the orbital plane, which will certainly not be correct if, as expected, the accretion region (the assumed source of the irradiation) is out of the orbital plane. However, if the bulk of the accretion luminosity arises close to the white dwarf surface, this asymmetry will be relatively small, and is unlikely to be resolvable using the Na I doublet, which has a fairly large intrinsic width. The addition of an extra parameter, to determine the latitude of the centre of the spot, would probably only degrade the entire fit, and make the correction to the radial velocity amplitude less reliable.

Although it gives no clue to the real latitudinal variations, the model does readily give both any longitudinal asymmetry about the L_1 point and the size of the affected area. It is also simple and requires only three fitting parameters, which allows rapid convergence to the best fit. At present the radial velocity data are not accurate enough to pick out small spots on the surface, so the model attempts only to locate the one main area of irradiation. We have chosen the Na I doublet as the line with which to map the surface irradiation, because Brett & Smith (1993) have shown that the Na I flux deficit decreases with increasing irradiation; the sodium is ionized by the incident flux.

The relative strength of the Na I doublet over the surface is parametrized by

$$I(\theta,\phi)=\begin{cases} I_0 - A\sin\theta\cos\dfrac{\phi-\phi_0}{2B} & \left|\dfrac{\phi-\phi_0}{2B}\right|<\dfrac{\pi}{2} \\ I_0 & \text{otherwise,} \end{cases} \tag{2}$$

where θ and ϕ are the standard spherical polar and azimuthal angles. The angle θ is measured from the positive z axis, and ϕ is measured anticlockwise from the positive x axis in the xy plane. (Note: the positive x axis is towards the primary star. Also, the equatorial angle ϕ is related to the orbital phase φ via $\phi=\pi-2\pi\varphi$.) Here I_0 represents the unperturbed flux deficit of the Na I doublet, A (which is positive) denotes the maximum decrease in the flux deficit on the surface of the secondary star, B is the equatorial extent of the spot as a fraction of the circumference of the star, and ϕ_0 is the angle measured anticlockwise from the L_1 point to the centre of the heated region. When $I(\theta,\phi)$ is less than zero, then it is set to zero (this can happen if A is larger than I_0). The Na I doublet is weakest at $\phi=\phi_0$, $\theta=\pi/2$, which is supposed to be the place where the irradiation is strongest.

The choice of a $\cos\phi$ term to represent the longitudinal variation about this point is also justified on grounds of simplicity; given the distorted shape of the secondary star, it is certainly only a rough representation of reality, especially if $\phi_0\neq 0$. We believe that a more sophisticated representation would not yield a significantly more reliable map, given the quality of the data. The agreement of our simple model with the maximum entropy map given in Section 3.3 is some justification for this point of view.

For a given observational phase and inclination, a total spectral profile is generated by adding the Na I doublet profiles from each surface element ij, allowing for the radial velocity (Doppler shift) of the element and weighting each by its apparent area and flux deficit I_{ij}. For fuller details see Davey & Smith (1992) and Davey (1994).

The coefficients A, B and ϕ_0 are initially guessed, and a synthetic residual radial velocity curve, $V_{\rm syn}(\varphi)$, is obtained for the flux deficit distribution $I(\theta,\phi)$. The same orbital phases as the original observations are used, and the goodness-of-fit between the synthetic residual velocities and the observed residual velocities is calculated using the reduced χ^2 statistic

$$\chi^2_{\rm rv}=\frac{1}{N-3}\sum_{k=1}^{N}\left[\frac{V_{\rm res}(k)-V_{\rm syn}(k)}{\sigma_{\rm rv}(k)}\right]^2. \tag{3}$$

Here $\sigma_{\rm rv}(k)$ is the rms deviation for each observation k at orbital phase $\varphi(k)$. Since this is not known in general, the values of $\sigma_{\rm rv}(k)$ are taken to be the same, usually $\sigma_{\rm e}$ from the elliptical fit, for all phases. The fitting coefficients are suitably corrected until the smallest value of χ^2, i.e., the best fit, is reached and the convergence stops. At this stage one needs to determine whether the value of K_2 initially chosen was correct.

The observed eccentricity is now compared to the eccentricity of the model radial velocities. The value of K_2 used is then decreased if the model eccentricity is too low and increased if it is too high. For this new value of K_2 a new self-consistent value of q (if the period, M_2 and inclination are assumed fixed) has to be calculated, and A, B and ϕ_0 are again computed to minimize χ^2. Correction of K_2 proceeds in this iterative manner, with usually only two or three iterations required, until one achieves results consistent with the observations.

The errors for the model eccentricity were computed from an elliptical fit to the model radial velocities. This also gives the error in the semi-amplitude of the elliptical fit to the model radial velocities, which when combined with the observed error on $K_{\rm abs}$ (which is usually much larger) gives an error for the corrected K_2 value. The error on ϕ_0 is obtained by fixing ϕ_0 at various values around the optimal value and reminimizing χ^2 with just A and B allowed to vary. A plot of $\chi^2_{\rm rv}$ against ϕ_0 is shown in Fig. 1 for AM Her. A 1σ

confidence level corresponds to $\chi^2_{\rm min}+1/(N-2)$ (where N is the number of observations and there are only two free parameters now); 2σ corresponds to $\chi^2_{\rm min}+4/(N-2)$, etc. (Press et al. 1992).

2.3 Surface mapping from flux deficits

Wade & Horne (1988) observed in Z Cha that the Na I doublet and TiO flux deficits varied with phase, so one can also use the observed variation of the sodium doublet line strength to put further constraints on the surface irradiation map.

The Na I doublet flux deficit is derived from the original spectra using

$$fd(\text{Na I}) = \int_{8165}^{8215} [c(\lambda) - f(\lambda)]\, \mathrm{d}\lambda, \tag{4}$$

where $f(\lambda)$ is the profile of the Na I doublet, and $c(\lambda)$ is the mean continuum level. The continua were fitted using the routine POLFIT (written by T. R. Marsh) which fits a fifth-order polynomial to the data; having obtained the rms deviation for the fit, the routine then rejects any points that lie more than 2.5 times the rms value away from the fit. As an example, a co-added spectrum of AM Her generated from six spectra around phase 0.0 is shown in Fig. 2 with its continuum fit. The spectrum was fitted only in the region 7850 to 8300 Å, because we were interested only in the region around the sodium doublet. Also, the data points marked by an 'x' were excluded from the fit.

If good flux deficit data are available for any system, then the surface distribution can be mapped using the same method as that used to model the residual radial velocities. Ideally, this requires spectrophotometric data, whereas the radial velocity maps can be made without spectrophotometry. As before, the surface of the secondary star is divided into small elements, and a Na I doublet line strength ascribed to each using the formula given in equation (2). Again the surface map is used to generate synthetic spectra, from which the flux deficit is calculated using equation (4). Now, rather than using the radial velocities, the goodness-of-fit between the model flux deficits and the observed flux deficits is calculated using

$$\chi^2_{\rm fd} = \frac{1}{N-3} \sum_{k=1}^{N} \left[\frac{fd_{\rm obs}(k) - fd_{\rm syn}(k)}{\sigma_{\rm fd}(k)} \right]^2. \tag{5}$$

Here $\sigma_{\rm fd}(k)$ is the rms deviation for each observation k at orbital phase $\varphi(k)$ and can be estimated from the rms deviation found from the continuum fit to the observed spectra. As before, the coefficients A, B and ϕ_0 are suitably corrected until the smallest value of χ^2, i.e., the best fit, is achieved and the convergence stops.

From this resulting surface map one can then get predicted radial velocity corrections that should be applied to the observed radial velocities. The advantage of this method is that an initial estimate of K_2 for the system is not required. The radial velocity corrections will depend on the orbital inclination, the period and also weakly on the secondary mass and mass ratio, so these might need to be estimated initially. However, the method does give a rough estimate of the inclination of the system when it is not eclipsing, although the symmetry assumptions made in the modelling prevent any precise conclusions.

3 RESULTS FOR AM HER

3.1 Determination of the inclination

Although we have no spectrophotometric measurements for AM Her, the continuum flux (Fig. 3) seems to vary smoothly and consistently over the two nights. The dip in the continuum flux around phase 0.5 could be caused by obscuration of the front face of the secondary star by the gas stream and magnetospheric impact hotspot, or by the geometrical projection of the accretion stream; both explanations suggest an angle of inclination higher than the value of 35° usually quoted (Brainerd & Lamb 1985).

The radial velocity and flux deficit data were fitted simultaneously, using the method described in Section 2, with a range of system inclinations to try to estimate the value that gives the best results. These results are shown in Fig. 4 and

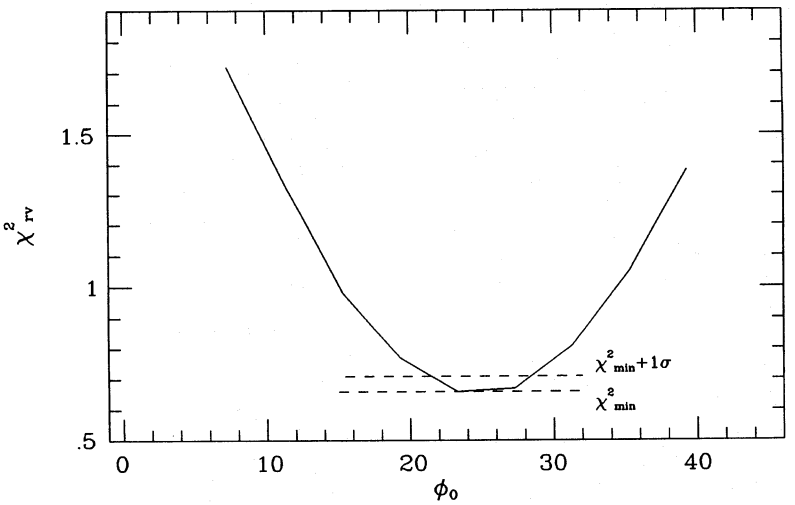

Figure 1. Minimum χ^2 plot for AM Her used for computing the error on ϕ_0.

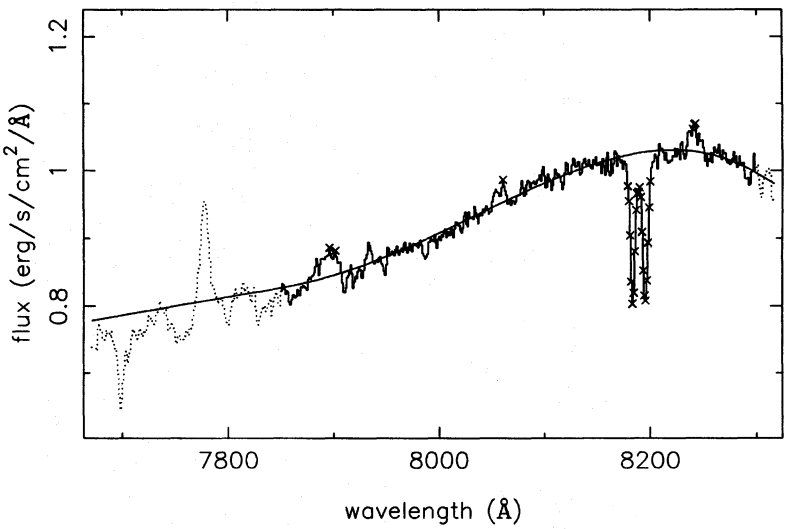

Figure 2. Co-added spectrum of AM Her produced from six observations around phase zero, with the continuum fit obtained from the routine POLFIT. The dotted parts of the spectrum were excluded from the fit. Points with more than a 2.5σ deviation from the fit, marked with an 'x', were also excluded from the fit.

clearly show that for $i \gtrsim 45°$ the fit improves significantly. Unfortunately, the inclination cannot be determined particularly accurately because the data are equally well fitted for inclinations greater than 45° by using a surface line strength distribution that does not decrease so markedly at the front of the star. None the less, despite the assumptions in the modelling, which make firm conclusions about the inclination rather doubtful, the large variation in flux deficit with phase would be hard to understand if the inclination were as low as 35°. An upper limit on the inclination of about 60° to 70° can be inferred from the lack of eclipses of the L_1 point or gas stream observed around phase zero. So an inclination of between 45° and 60° would be the preferred value from this work. This is also consistent with $i = 52°$ obtained by Wickramasinghe et al. (1991).

3.2 Surface maps

The data were now fitted for an orbital inclination of 50°, period = 3.094 h, $M_2 = 0.26\ M_\odot$ (from the main-sequence assumption) and $q = 0.6$, where $q = M_2/M_1$. These values are in good agreement with the parameter ranges derived by Southwell et al. (1995). The results are plotted in Fig. 5 for the flux deficit data and Fig. 7 for the radial velocity data, and are also summarized in Table 1. The corresponding surface maps are shown in Figs 6 and 8 respectively. The view of the secondary star is from the top looking down the axis of rotation (z axis) with the white dwarf to the right along the x axis. The units on the axes are in terms of the binary separation for this system.

As can be seen in Fig. 6, the resulting surface map from the Na I flux deficit data compares well with that in Fig. 8 obtained from the radial velocity data. Table 1 shows that the model eccentricity is much closer to the observed value of 0.068 ± 0.010 when $i = 50°$ than when $i = 35°$; the values of χ^2 for the maps are also lower for the higher inclination.

The surface maps obtained are relatively unaffected by choosing K_2 in the range allowable for consistency with the observed eccentricities. In particular, the phase angle of the terminator does not appear to change significantly as K_2 is varied. Since the strength of the Na I doublet is related to the temperature at the surface (Brett & Smith 1993), these plots also give an indication of the temperature distribution over the secondary star.

Here the irradiation is by the white dwarf and accretion column only and might be expected to be almost exactly symmetrical about the L_1 point. However, for AM Her the direction of the magnetic pole of the white dwarf, and hence the likely direction of the gas stream, is given as $\beta = 61°$ and $\psi = 31°$ (Cropper 1988), where β is the angle measured downwards from the axis of rotation, and ψ is the angle measured anticlockwise from the line joining the white dwarf to the secondary star. This geometry is shown in Fig. 9 and suggests that the incoming accretion column is blocking radiation produced very close to the white dwarf, thereby shielding an area on the leading side of the secondary star. Indeed, observations of GQ Mus (Shaham 1993), also an AM Her type system, show irradiation of the front face of the secondary star. In that system there is a shadow on the red dwarf star around the L_1 point (of approximately 40° in extent) that is thought to be caused by flux from the accretion column being unable to radiate directly towards the secondary star because of the incoming gas stream.

3.3 Maximum-entropy reconstruction of surface features

Another method for identifying features on the surface of the secondary star is maximum-entropy reconstruction (using the MEMSYS package of Gull and Skilling: Skilling & Bryan 1984; Skilling & Gull 1985). The surface mapping routine used in this section was written by René Rutten and uses the original spectra directly to map surface features by modelling both the Doppler shifts and the line strength variations around the binary orbit (Rutten 1993; Rutten & Dhillon 1994). The advantage of this technique is that it does not use the measured radial velocities and flux deficits

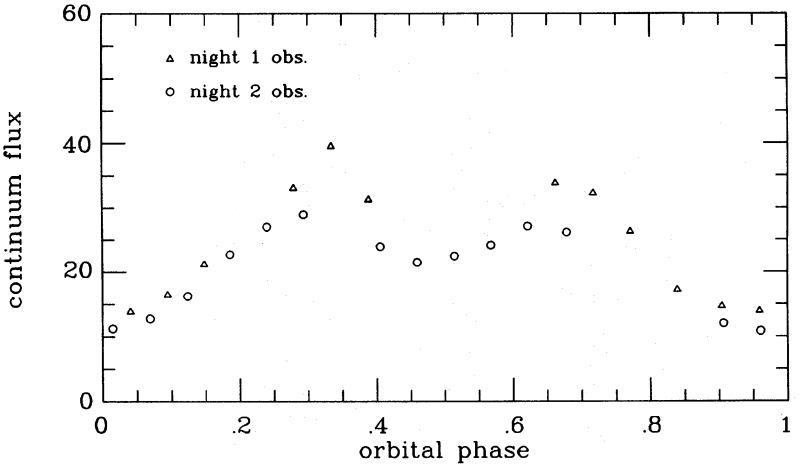

Figure 3. Continuum flux results for AM Her. The integrated continuum flux is given by $\int_{8165}^{8215} c(\lambda)\, d\lambda$ and is in arbitrary flux units.

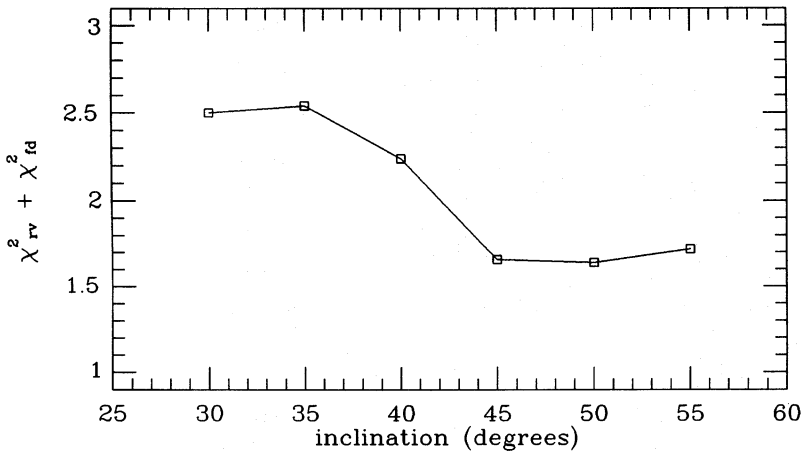

Figure 4. Plot of total χ^2 against a range of inclinations for the AM Her system.

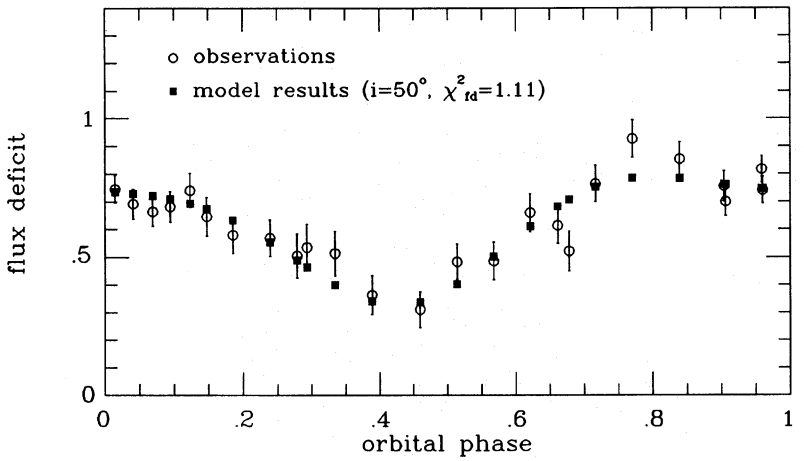

Figure 5. Flux deficit results for AM Her in which the model has fitted the flux deficits and an inclination of 50° has been used. The integrated flux deficit is in arbitrary units.

derived from the original spectra, but instead uses the actual variations in the line profile with phase and hence can, in theory, identify features covering only a few per cent of the surface. Indeed, this method has already been used for several years to map star spots on fast rotating magnetic stars (e.g., AB Dor: Collier Cameron & Unruh 1994). It has also been used to image accretion discs in CVs, where it is known as Doppler tomography or Doppler imaging (Marsh & Horne 1988).

The same binary system parameters as before were used

in the reconstruction, and an intrinsic Na I doublet line profile corresponding to $T_{\rm eff}=3000$ K was used as the mapping line. As can be seen in Fig. 10, the resulting surface map for AM Her agrees with those shown in Figs 6 and 8; a more detailed comparison (Davey 1994) shows that the agreement is good. Since no symmetry assumptions are involved in the maximum-entropy reconstruction, this agreement is a retrospective justification of our simple model; the quality of the data is not sufficient to resolve detail. The resolution is also limited (Davey 1994) by the relatively large intrinsic width (about 3 Å) of each component of the Na I doublet.

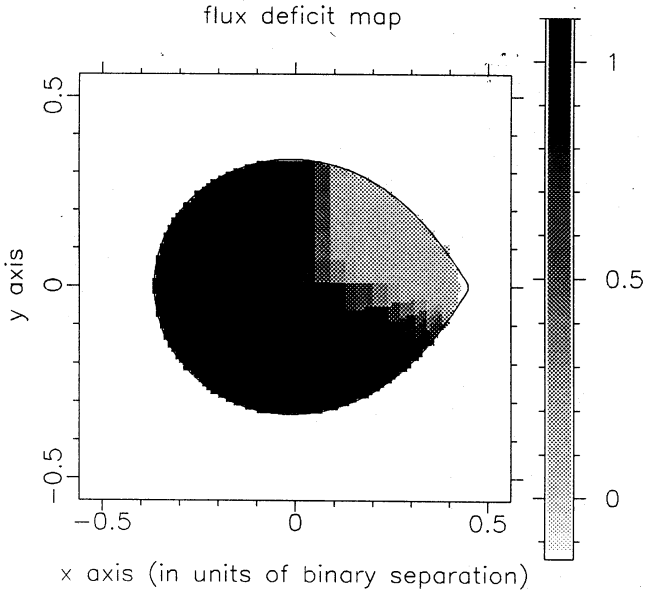

Figure 6. Surface map of AM Her showing the strength of the Na I doublet corresponding to the flux deficit results shown in Fig. 5. The light region is where the Na I doublet is weak. The view is from the axis of rotation (i.e., the z axis) looking down on to the top of the secondary star.

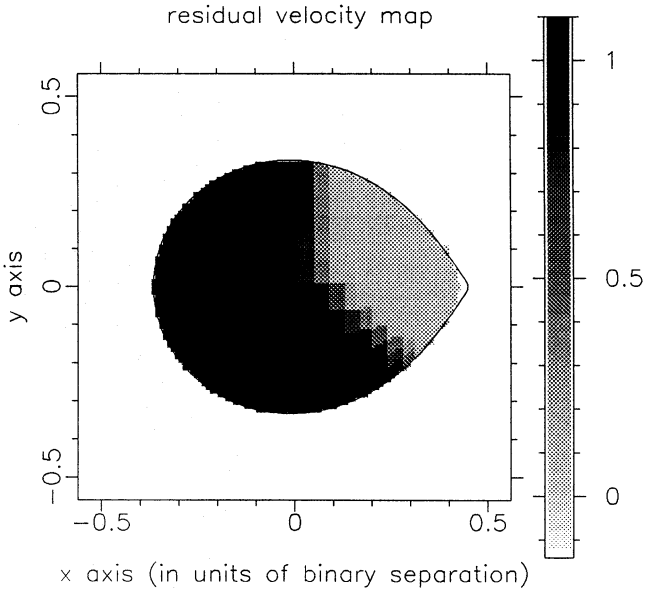

Figure 8. Surface map showing the strength of the Na I doublet corresponding to the radial velocity results shown in Fig. 7. The light region is where the Na I doublet is weak. The view is as in Fig. 6.

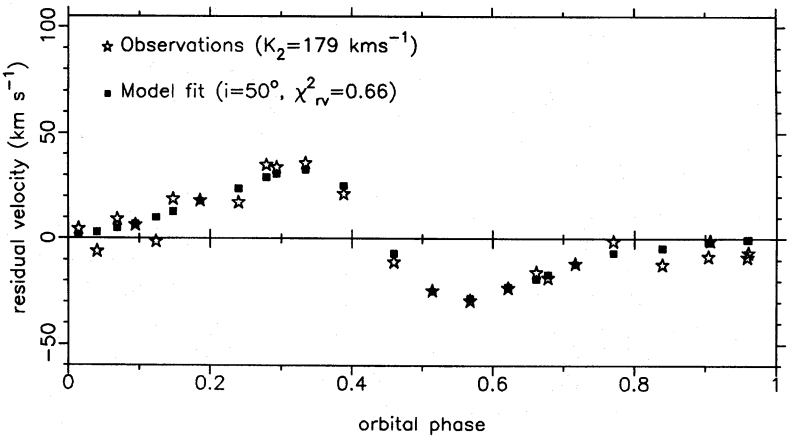

Figure 7. Residual radial velocity results for AM Her in which the model has fitted the radial velocity data and an inclination of 50° has been used.

Table 1. Radial velocity results for AM Her from mapping flux deficit data and residual velocity data.

	K_2	q	e	χ^2_{rv}	χ^2_{fd}	ϕ_0	extent
$i=35°$ rv model	174 ± 2	0.37	0.029 ± 0.002	1.80	2.54	$+22°\pm4°$	46%
$i=50°$ rv model	179 ± 2	0.60	0.063 ± 0.006	0.66	1.65	$+25°\pm4°$	35%
$i=50°$ fd model	179 ± 2	0.60	0.060 ± 0.007	0.95	1.11	$+30°\pm5°$	29%

Unfortunately, as Rutten & Dhillon (1994) point out, maximum-entropy optimization is a non-linear procedure, and therefore uncertainties in the resulting map cannot be derived directly from uncertainties in the data. A proven method of obtaining errors in the surface map is to employ a Monte Carlo technique, but the large number of reconstructions that one would need to perform would at present require a prohibitively large amount of computing time. With increasing computing power, this will cease to be a problem, and Roche tomography promises to become a powerful tool for studying the surface of the secondary star.

The principal disadvantage of the technique at present, and the reason that we have not adopted it wholesale for our mapping of secondaries, lies in the feature that is also its strength: its use of individual line profiles. Absorption lines from the secondary are generally weak, and the signal-to-noise (S/N) ratio in the lines is relatively low, making the variation in line profile with orbital phase rather noisy. Numerical experiments (Davey 1994) suggest that a S/N ratio of 50 or more is required to make effective use of maximum-entropy mapping; the data presented here for AM Her have a S/N ratio of about 10 and are only capable of resolving the large-scale features that we have modelled with the one-spot model. It therefore seems better with low S/N data to include some restriction in the model, such as our one-spot assumption, since allowing a free choice for the model may throw up low S/N features whose reality is hard to judge.

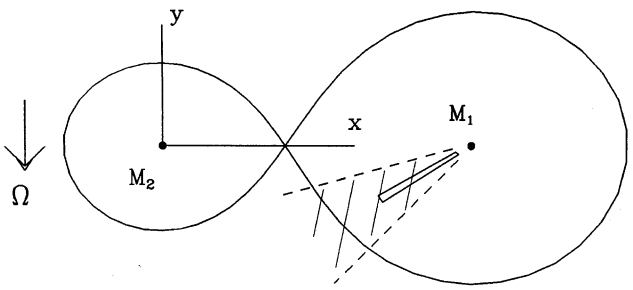

Figure 9. Sketch of the magnetic cataclysmic variable AM Her, showing the direction of the accretion pole.

Obtaining larger S/N ratios is always difficult for CVs, given the intrinsic faintness of the secondary and the need for short exposures to avoid velocity smearing. The orbital variation also requires spectrophotometry for optimal results (as does our use of flux deficits). Further, the maximum-entropy technique is vulnerable to contamination of the line profile by other sources of light; our technique is not quite so vulnerable to this effect, because of the extra assumption about the light distribution. It is our view that, until good error estimates can be obtained for maximum-entropy maps, there is no great advantage in using this technique except for very high-quality data, since the reality of any features other than a simple single spot around the

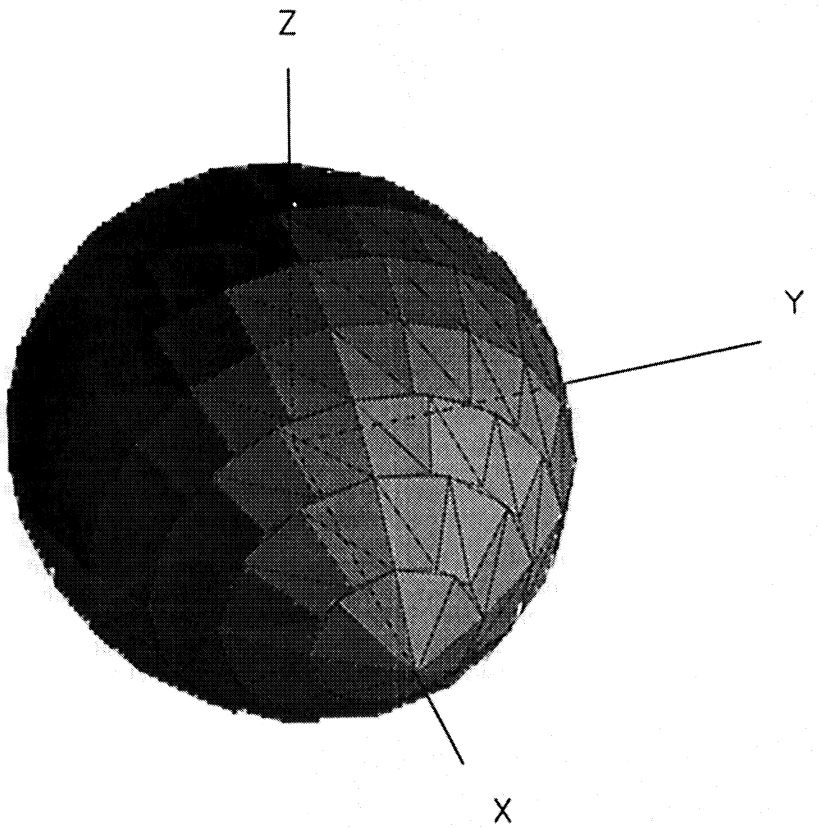

Figure 10. Maximum-entropy map for AM Her in which a 3000-K Na I doublet template has been used as the mapping line, and an orbital inclination of 50° has been assumed. The plot shows a 3D view from phase 0.55.

centre of irradiation would be in doubt. Our one-spot model is a computationally simple way of determining the correction to the radial velocity amplitude, which was the original aim of this work.

4 CONCLUSIONS

When studying the red dwarf star in CV systems irradiation can be expected from the white dwarf and accretion flow, and one needs to allow for this in order to get corrected values for the orbital velocity of the secondary star. A failure to correct K_2 when necessary can lead to quite large errors in the mass ratio and incorrect masses. However, a correction of K_2 solely from the observed eccentricity in the radial velocity curve can sometimes give the wrong results. A better way is to compute the surface line strength map that best fits the radial velocity data, and this also has the advantage of giving an idea of the size and position of surface features. The radial velocity data can also help to constrain system parameters, and for AM Her suggest an inclination of between 45° and 60°.

Obtaining spectrophotometric data is very important, since it provides surface distribution information that is independent of, but clearly related to, the radial velocities derived from the spectra. In the AM Her system the phase-resolved spectra indicate that the system is being irradiated mainly to one side of the L_1 point, because of the geometry of the gas stream and accretion column, as shown in Fig. 9. Wickramasinghe et al. (1991) propose a slightly different gas stream geometry for AM Her in which there are two accretion regions, as sketched in Fig. 11. Their model has one main accretion region above the orbital plane, 140° anticlockwise from the line of centres, which extends about 8° in phase. The second is below the plane, about 170° away from the line of centres and 20° to 30° in extent. Since the positions of the accretion regions are both more than 90° away from the line of centres, there would seem to be no reason why the white dwarf and accretion column would not have a 'clear view' of the whole of the front face of the secondary star. This would therefore be unlikely to give the asymmetrical maps of AM Her (e.g., Fig. 6), whereas the magnetic field geometry proposed by Cropper (1988) does seem to be fully consistent. Of course, this conclusion is tentative, since the structure of the accretion stream, especially near the threading region, is complex and uncertain, and the stream itself may be doing the shadowing.

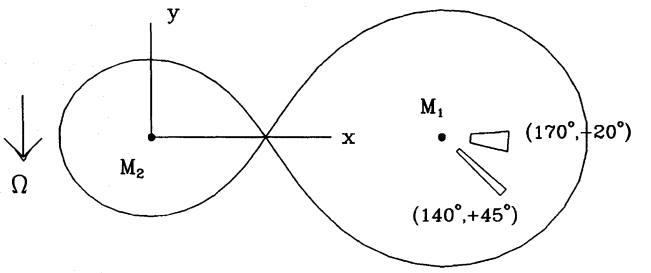

Figure 11. Sketch of two-pole accretion model for AM Her of Wickramasinghe et al. (1991).

ACKNOWLEDGMENTS

We thank Jackie Martin and Derek Jones for the use of the surface mapping code and the observational data, René Rutten for the use of his Roche tomography program and for much valuable assistance, and Sandi Catalán, Karen Southwell and Martin Still for many interesting discussions.

This work was produced at the University of Sussex Starlink node. SCD acknowledges receipt of an SERC studentship. We are also grateful to the referee for a detailed and helpful report, which has improved the presentation.

REFERENCES

Brainerd J. J., Lamb D. Q., 1985, in Lamb D. Q., Patterson J., eds, Proc. of the 7th North American Workshop on Cataclysmic Variables and Low Mass X-Ray Binaries. Reidel, Dordrecht, p. 247
Brett J. M., Smith R. C., 1993, MNRAS, 264, 641
Collier Cameron A., 1992, in Byrne P. B., Mullan D. J., eds, Surface Inhomogeneities on Late-Type Stars. Springer-Verlag, Berlin, p. 33
Collier Cameron A., Unruh Y. C., 1994, MNRAS, 269, 814
Cropper M., 1988, MNRAS, 231, 597
Davey S. C., 1994, DPhil thesis, Univ. Sussex
Davey S. C., Smith R. C., 1992, MNRAS, 257, 476
Friend M. T., Martin J. S., Smith R. C., Jones D. H. P., 1988, MNRAS, 233, 451
Marsh T. R., Horne K., 1988, MNRAS, 235, 269
Martin J. S., 1988, DPhil thesis, Univ. Sussex
Martin J. S., Friend M. T., Smith R. C., Jones D. H. P., 1989, MNRAS, 240, 519
Press W. H., Teukolsky S. A., Vetterling W. T., Flannery B. P., 1992, Numerical Recipes: The Art of Scientific Computing, 2nd edn. Cambridge Univ. Press, Cambridge, p. 692
Rutten R. G. M., 1993, in Regev O., Shaviv G., eds, Cataclysmic Variables and Related Physics. Annals of the Israel Physical Society, Vol. 10. IoPP, Bristol/IPS, Jerusalem, p. 309
Rutten R. G. M., Dhillon V. S., 1994, A&A, 288, 773
Shaham J., 1993, in Regev O., Shaviv G., eds, Cataclysmic Variables and Related Physics. Annals of the Israel Physical Society, Vol. 10. IoPP, Bristol/IPS, Jerusalem, p. 53
Skilling J., Bryan R. K., 1984, MNRAS, 211, 111
Skilling J., Gull S. F., 1985, in Smith C. R., Grandy W. T., eds, Maximum Entropy and Bayesian Methods in Inverse Problems. Reidel, Dordrecht, p. 83
Southwell K. A., Still M. D., Smith R. C., Martin J. S., 1995, A&A, 302, 90
Wade R. A., Horne K., 1988, ApJ, 324, 411
Wickramasinghe D. T. et al., 1991, MNRAS, 251, 28